



1 Aridification signatures from middle–late Eocene pollen indicate 2 widespread drying across the Tibetan Plateau after 40 Ma

3 Qin Yuan^{a,b,c,d,*}, Natasha Barbolini^{e,f}, Catarina Rydin^{e,g}, Dong-Lin Gao^{a,b}, Hai-Cheng Wei^{a,b}, Qi-Shun
4 Fan^{a,b}, Zhan-Jie Qin^{a,b}, Yong-Sheng Du^{a,b}, Jun-Jie Shan^{a,b,c}, Fa-Shou Shan^{a,b}, Vivi Vajda^d

5 ^a Key Laboratory of Comprehensive and Highly Efficient Utilization of Salt Lake Resources, Qinghai Institute of Salt Lakes,
6 Chinese Academy of Sciences, Xining, China

7 ^b Qinghai Provincial Key Laboratory of Geology and Environment of Salt Lakes, Qinghai Institute of Salt Lakes, Chinese
8 Academy of Sciences, Xining, China

9 ^c University of Chinese Academy of Sciences, Beijing 100049, China

10 ^d Swedish Museum of Natural History, Stockholm, Sweden

11 ^e Department of Ecology, Environment and Plant Sciences and Bolin Centre for Climate Research, Stockholm University, SE-
12 106 91 Stockholm, Sweden

13 ^f Department of Ecosystem and Landscape Dynamics, Institute for Biodiversity and Ecosystem Dynamics, University of
14 Amsterdam, 1098 XH The Netherlands

15 ^g The Bergius Foundation, The Royal Swedish Academy of Sciences, Box 50005, SE-104 05 Stockholm, Sweden

16 Correspondence to: Natasha Barbolini (barbolini.natasha@gmail.com)

17 **Abstract.** Central Asia experienced a number of significant elevational and climatic changes during the Cenozoic, but much
18 remains to be understood regarding the timing and driving mechanisms of these changes, as well as their influence on
19 ancient ecosystems. Here we describe the palaeoecology and palaeoclimate of a new section from the Nangqian Basin in
20 Tibet, northwestern China, here dated as late Lutetian–Bartonian (late middle–late Eocene) based on our palynological
21 analyses. Located on the east-central part of the Tibetan Plateau, this section is excellently placed for better understanding
22 the palaeoecological history of Tibet following the India-Asia collision. Our new pollen record reveals that a strongly



23 seasonal steppe-desert ecosystem characterised by drought-tolerant shrubs, diverse ferns and an underlying component of
24 broad-leaved forests existed in east-central Tibet during the Eocene, influenced by a southern monsoon. Warming during the
25 Middle Eocene Climatic Optimum only prompted a temporary vegetation response, while a drying signature in our pollen
26 record after 40 Ma demonstrates that proto-Paratethys sea retreat caused widespread long-term aridification across the
27 plateau. To better distinguish between local climatic variation and farther-reaching drivers of Central Asian palaeoclimate
28 and elevation, we correlated key palynological sections across the Tibetan Plateau by means of established radioisotopic ages
29 and biostratigraphy. This new palynozonation illustrates both intra- and inter-basinal floral response to plateau uplift and
30 global climate change during the Paleogene, and provides a framework for the age assignment of future palynological studies
31 in Central Asia. Our work highlights the ongoing challenge of integrating various deep time records for the purpose of
32 reconstructing palaeoelevation, indicating that a multiproxy approach is vital for unravelling the complex uplift history of the
33 Tibetan Plateau and its resulting influence on Asian climate.

34

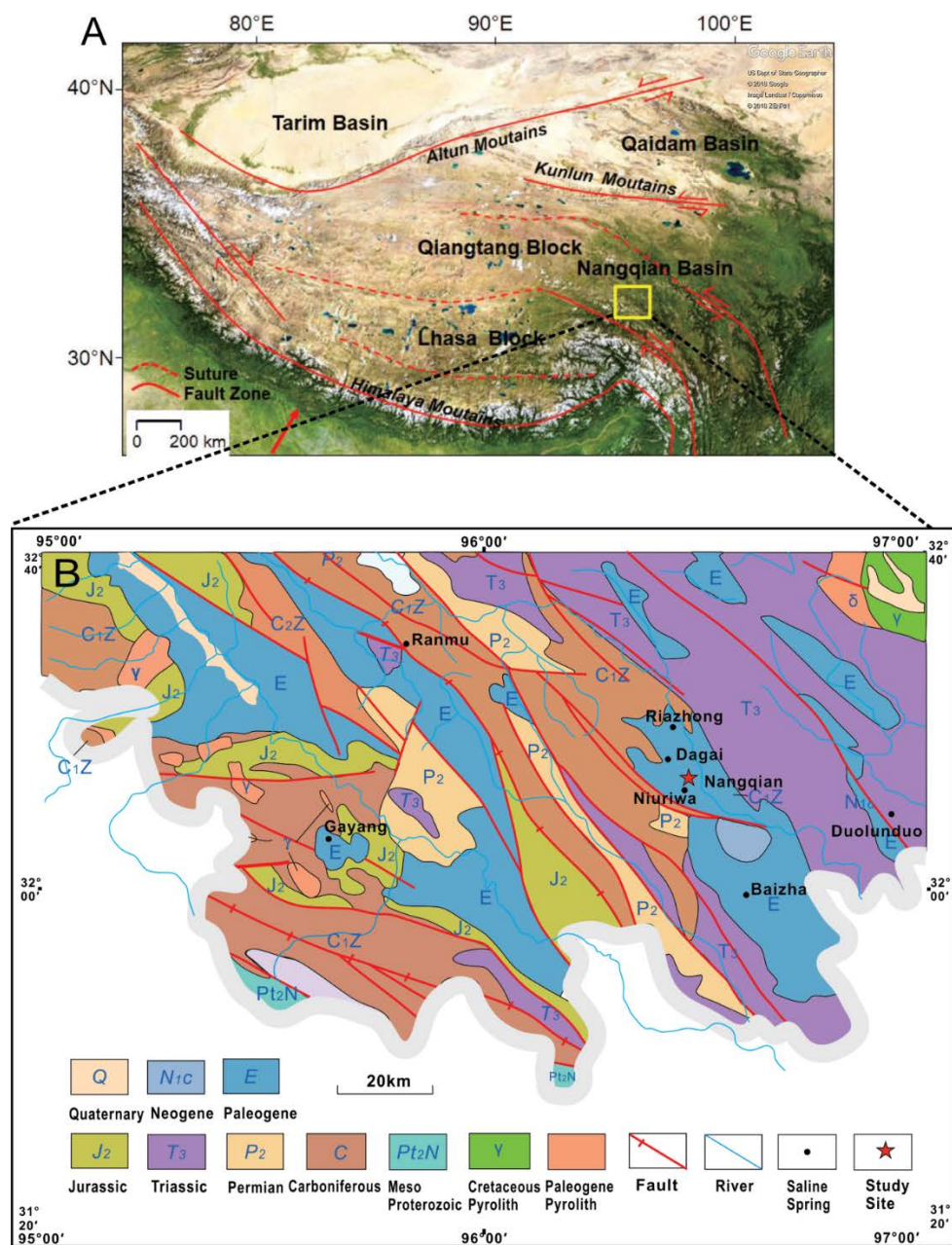
35 **1. Introduction**

36 A series of major geological events occurred during the Cenozoic, which led to a fundamental change in the global
37 climate (Zachos et al., 2001). The most important events include the formation of the polar ice cap (e.g., DeConto and
38 Pollard, 2003; Pagani et al., 2011), regression of the proto-Paratethys Sea from Eurasia (Abels et al., 2011; Bosboom et al.,
39 2014; Caves et al., 2015; Bougeois et al., 2018; Kaya et al., 2019; Meijer et al., 2019), and uplift of the Tibetan Plateau
40 (Dupont-Nivet et al., 2007, 2008; Molnar et al., 2010; Miao et al., 2012; Hu et al., 2016; Li et al., 2018). Today the Tibetan
41 Plateau (TP) is the highest elevated plateau in the world and was formed as a result of the collision between the Indian and
42 Asian continents (Molnar and Tapponnier, 1975; Aitchison and Davis, 2001; Wang, C.S., et al., 2008; Wang, C.W., 2014; Xia
43 et al., 2011; Aitchison et al., 2011; Zhang et al., 2012). Previous studies indicate that retreat of the proto-Paratethys Sea and
44 the uplift of the TP as well as other ranges north of the plateau, such as the Altai, Sayan, and Hangay (Caves et al., 2014),
45 may have been responsible for monsoon intensification and aridification across the Asian continental interior in the



46 Paleogene, although the timing of these mechanisms, and their roles in forcing climate dynamics, are still debated (Caves et
47 al., 2015; Spicer, 2017). In particular, a lack of consensus exists regarding the onset of Asian aridification, whether it was a
48 Paleogene or Neogene phenomenon, and its relationship with TP uplift (e.g., Dupont-Nivet et al. 2007; Xiao et al., 2010;
49 Miao et al., 2012; Caves et al., 2015; Liu et al., 2016; Wang et al., 2018; Li et al., 2019; Paeth et al., 2019).

50 The uplifting, large-scale thrusting and striking of the TP caused several Paleogene intracontinental basins to form
51 within the northern TP, including the Nangqian Basin. Situated in the Yushu area (Fig. 1), this basin lies directly above the
52 Lhasa terrane, which comprised part of NE Gondwana in the Late Triassic to Early Jurassic and formed through a
53 subduction–accretion process similar to that of the later India–Asia collision (Liu et al., 2009). Subsequent to its formation,
54 the Nangqian Basin was infilled with non-marine sedimentary deposits (Wang et al., 2001; 2002), and is now a key site for
55 understanding the Cenozoic tectonics, palaeoelevation and paleoclimatic changes that took place on the TP since the
56 collision of the Indian and Asian tectonic plates (Gupta et al., 2004; Molnar, et al., 2004; Wang et al., 2001). Previous
57 palynological studies from this part of the plateau revealed a relatively dry climate with brief humid intervals in the late
58 Eocene, dominated by drought-tolerant (xerophytic) and salt-tolerant (halophytic) steppe-desert vegetation (Wei, 1985; Yuan
59 et al., 2017). This climate and palaeoflora were very similar to contemporaneous plateau ecosystems further to the north,
60 such as the Xining (Dupont-Nivet et al. 2007, 2008; Hoorn et al., 2012) and Hoh Xil (Liu et al., 2003; Miao et al., 2016)
61 basins, demonstrating the potential for these successions to be biostratigraphically correlated. Oxygen isotope records
62 indicate that northward of the central TP, the westerlies acted as the dominant moisture source since at least the early Eocene
63 (Caves et al., 2015). In contrast, southeastern Tibet seems to have experienced a more humid climate hosting widespread
64 conifer and warm-temperate broad-leaved forests (Li et al., 2008; Su et al., 2018), likely influenced by a Paleogene ITCZ-
65 driven monsoon system similar to the modern Indonesia–Australian Monsoon (I-AM; Spicer et al., 2017). Moreover, these
66 southern Tibetan Eocene floras display a modern aspect that is quite different to more ancestral steppe vegetation hosted in
67 the northern TP.



68

69 Figure 1: (A) Topographic map of the Tibetan Plateau (TP) with major basins indicated. Base map US Dept. of State Geographer,
 70 ©2018 Google, Image Landsat/Copernicus ©2018 ZENRIN; (B) Simplified geologic map of the study area in the Nangqian Basin
 71 (after Han et al., 2018).



72 The extent and timing of mechanisms that promoted somewhat different floras south and north of the Tibetan–
73 Himalayan orogen remain poorly understood, with Licht et al. (2014) reporting marked monsoon-like patterns in both
74 regions during the Eocene, utilising records from northwest China and Myanmar. The role of TP uplift also remains unclear,
75 with contrasting models of plateau evolution supported by various tectonic, isotopic, modelling, and biological evidence
76 (e.g., Mulch and Chamberlain, 2006; Rowley and Currie, 2006; Ding et al., 2014; Li et al., 2015; Jin et al., 2018; Botsyun et
77 al., 2019; Su et al., 2019; Valdes et al., 2019; Shen & Poulsen, 2019 and see summaries in Spurlin et al., 2005; Wang et al.,
78 2014; Spicer, 2017). Accordingly, further stratigraphic and paleoenvironmental studies of the sedimentary successions within
79 these basins are necessary to provide clarification on local vs. regional climatic changes experienced as a result of uplift,
80 global cooling, and progressive aridification in Central Asia during the Paleogene. The location of the Nangqian Basin on the
81 east-central part of the TP provides an ideal locality for testing the influence of these mechanisms on Asian
82 palaeoenvironments and climates. We selected the Ria Zhong (RZ) section in the Nangqian Basin for palynological analyses,
83 and correlated this section with previous studies from this and other TP basins. These new results better constrain the
84 biostratigraphy of Paleogene successions across the plateau, and provide new information on the depositional environment,
85 and elevational and climatic changes in eastern Tibet during the Eocene. We further synthesise results previously published
86 in Chinese journals, making these results accessible for an international audience.

87

88 **2. Geological background, stratigraphy and lithofacies**

89 The Nangqian Basin is located on the border between the Qinghai Province and Tibet Autonomous Region at an
90 elevation of approximately 4500–5000 m and characterized by a continental seasonal monsoon climate, with long, cold
91 winters, and short, rainy, and cool to warm summers (Yuan et al., 2017). Most of the annual precipitation occurs from June to
92 September, when on average, most days in each month experience some rainfall (Qinghai BGMR, 1991). The region
93 presently hosts alpine steppe and meadow characterised by Cyperaceae, Asteraceae, Amaranthaceae, and Poaceae, as well as
94 conifer and broad-leaved forests dominated by conifers such as *Pinus*, *Picea*, *Abies*, *Tsuga*, and deciduous angiosperms such



95 as *Quercus* (oak), and *Betula* (birch) although intensive logging has markedly contracted these forests to steep slopes and
96 remote areas (Herzschuh, 2007; Baumann et al., 2009).

97 Although the timing of the Indo-Asian collision remains uncertain (e.g., Xia et al., 2011; Zhang et al., 2012; Wang et
98 al., 2014), its initiation formed north-eastward extrusion facilitated by motion along a series of contraction deformation and
99 strike-slip faults in eastern Tibet, including the Yushu–Nangqian thrust belt and the Jinshajiang strike-slip fault system (Fig.
100 1; Hou et al., 2003; Yin and Harrison, 2000; Spurlin et al., 2005). The Nangqian Basin is one of four sedimentary basins in
101 the Nangqian–Yushu region that formed during Paleogene contraction (Horton et al., 2002), ~80 km-long in S–N direction,
102 and 15 km-wide in E–W direction, and situated in the eastern part of the Qiangtang terrane (Fig. 1; Hou et al., 2003). The
103 tectonic evolutionary history of the area includes an early stage extrusion thrust foreland basin, a middle stage strike-slip
104 foreland basin, and the late stage extrusion strike-slip foreland basin (Wang et al., 2001, 2002; Mao et al., 2010; Jiang et al.,
105 2011).

106 Paleozoic, Mesozoic, and Paleogene sedimentary rocks exposed along the Yushu–Nangqian traverse include
107 Carboniferous–Triassic marine carbonates and minor clastic units overlain by Jurassic, Cretaceous, and Paleogene red beds
108 (Liu, 1988; Qinghai BGMR, 1991). The southern area mainly comprises the Carboniferous Zhaduo Group (C¹zd), whereas
109 the northern area is dominated by younger strata comprising the Upper Triassic Jieza Group (T³jz; Qinghai BGMR, 1991).
110 Our study concentrated on the Cenozoic gypsum-bearing Gongjue Formation, which unconformably overlies Carboniferous–
111 Triassic rocks and may be conformable with underlying Upper Cretaceous strata (Qinghai BGMR, 1983a, 1983b, 1991). It is
112 divided into five lithological units (Eg¹–Eg⁵), from bottom to top. Eg¹ comprises shallow lacustrine facies reaching a
113 thickness of ca. 400 m, which lie unconformably on a basement of Carboniferous–Permian sedimentary rocks. The strata in
114 units Eg², Eg⁴, and Eg⁵ were mainly formed in an alluvial environment with rapid sedimentation rates, with strata reaching a
115 thickness of ca. 530 m, 1100 m, and 2500 m respectively.

116 The focus of this study is the Eg³ unit which has a more complex depositional history; it is the thickest (reaching 3500
117 m) of the five units, and the most widely distributed unit in the Nangqian Basin. Eg³ is divided into three members: 1) the



118 Ri'Anongguo conglomerate member, which reaches a thickness of approx. 1300 m; 2) the Dong Y'ru sandstone member
119 with limestone beds, which reaches a thickness of 700–1000 m; and 3) the uppermost Gouriwa member, comprising
120 mudstones (generally developed as red beds) intercalated with gypsum and reaching 900–1200 m in thickness (Wang et al.,
121 2002). This latter member has been interpreted as being deposited in a fluviolacustrine environment under a range of climatic
122 conditions (Wang et al., 2001, 2002; Jiang et al., 2011). Based on palynological analyses and ostracod assemblages, these
123 mudstone-dominated successions (Eg³) have been dated as late Eocene to Oligocene in age (Wei, 1985; Yuan et al., 2017),
124 which is corroborated by 38–37 Ma ⁴⁰Ar/³⁹Ar ages from interbedded volcanic rocks in the uppermost strata of the Nangqian
125 Basin (Spurlin et al., 2005).

126 Though few palynological data currently exist from the Nangqian Basin (Wei, 1985; Yuan et al., 2017), palynology has
127 been extensively applied for biostratigraphic purposes, as well as to infer Cenozoic climatic changes, in basins across the TP,
128 including the Qaidam Basin (Xu et al., 1958; Zhu et al., 1985; Wang et al., 1999; Sun et al., 2005; Lu et al., 2010; Ji et al.,
129 2011; Miao et al., 2011, 2012, 2013a; Cai et al., 2012; Herb et al., 2015; Wei et al., 2015), Xining Basin (Dupont-Nivet et al.,
130 2008; Miao, 2010; Hoorn et al., 2012; Miao et al., 2013b; Bosboom et al., 2014), Hoh Xil Basin (Liu et al., 2003; Miao et al.,
131 2016), Tarim Basin (Sun et al., 1999; Zhu et al., 2005; Bosboom et al., 2011; Wang et al., 2013), and the Xigaze region of
132 Tibet (Li et al., 2019). Most of these studies are limited to the sedimentary successions within the foreland basins of the
133 northern TP, rendering it important to gather further data on central plateau basins that preserve a complex sequence of
134 Cenozoic deformation in relation to the Indo-Asian collision zone (Spurlin et al., 2005). Furthermore, correlation of the
135 above-mentioned northern successions with our new section from the Nangqian Basin (presented in Section 5.1) is valuable
136 for advancing understanding of differences in vegetational composition across the TP, as well as the paleoenvironmental and
137 climatic signals recorded by these ecosystems.

138

139 3. Materials and Methods

140 In this study, the RZ section located in the northwestern part of the Nangqian Town (N32°12'10", E96°27'19.42",



141 altitude 3681 m) was sampled for sedimentological and palynological analyses (Fig. 1A). The RZ section is a ca. 260 m thick
142 portion of the Gongjue Formation where it represents the uppermost Gouriwa Member of the Eg³ unit (Fig. S1). The
143 sediments mainly comprise lacustrine facies represented by red mudstones and siltstones, intercalated with gypsum beds. A
144 more detailed description of the sedimentology, geochemistry, and palynofacies of the section are presented in a separate
145 manuscript (Yuan et al., in prep.). A total of 71 palynological samples were collected from mudstones or fine-grained
146 siltstones.

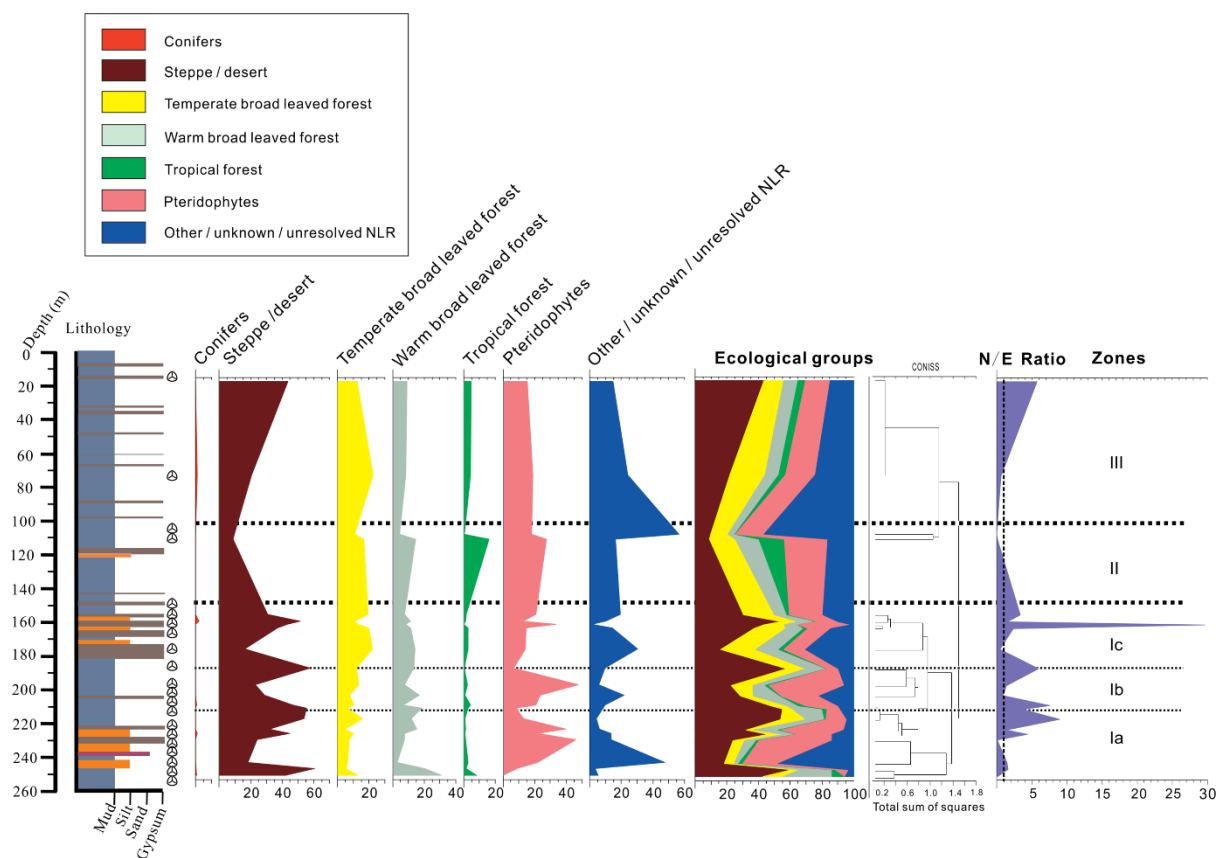
147 The samples were first treated with 36% HCl and 39% HF to remove carbonates and silicates and then sieved through a
148 10 µm nylon mesh. Subsequently, the residue was density separated using ZnCl₂ (density = 2.1). The organic residue was
149 mounted on microscopic slides in glycerin jelly. All slides were examined at the Swedish Museum of Natural History under a
150 Leica light-microscope (OLYMPUS BX51), and micrographs were taken of selected specimens. Slides and residues are
151 hosted at the Swedish Museum of Natural History, Stockholm, Sweden.

152 From each of the 21 productive samples > 200 grains were identified and counted, and the pollen diagrams (Fig. 2, Fig.
153 S2 & S3) plotted using TGView© and Tilia© 2.0 software (Grimm, 1991). Statistical analysis of the pollen assemblages was
154 conducted using CONISS (Constrained Incremental Sums of Squares cluster analysis), a multivariate agglomerative method
155 for defining zones hierarchically (Grimm, 1987). A stratigraphically constrained analysis was performed on pollen-
156 percentage values with square root transformation (Edwards & Cavalli Sforza's chord distance) which up-weights rare
157 variables relative to abundant ones, and is therefore particularly appropriate for pollen datasets (Grimm, 1987). Results of the
158 CONISS ordination on all taxa were presented as a dendrogram onto the pollen diagram (Fig. S2), and the ordination was
159 then repeated to test the robustness of the stratigraphic zones by excluding the “Other / Unknown / Unresolved NLR”
160 ecological group. Very similar zones were retained in the new cluster analysis (Fig. S3), increasing confidence that these
161 zones represent true changes in vegetation and climate dynamics recorded throughout the section. Both CONISS ordinations
162 were used in conjunction with the taxonomic and quantitative composition of the palynological assemblage, in order to
163 demarcate zones and subzones within the section.



164 **4. Results**

165 Recovery of palynomorphs was generally poor, with only 21 productive samples out of the 71 processed samples,
166 indicating a productivity ratio of 30%. Nevertheless, well-preserved palynological assemblages were recovered throughout
167 the section, enabling a representative portrayal of vegetation changes through time to be reconstructed. In total 26 spore and
168 81 pollen taxa (5 gymnosperm and 76 angiosperm morphospecies) were able to be identified, which are illustrated (Plate I,
169 II, III) and grouped into seven different Plant Functional Types (PFTs) that represent various ecological groups (Fig. 2).
170 Overall trends for the RZ section include rare conifers and a general dominance of steppe-desert pollen in all zones. Ferns
171 are abundant and diverse, particularly in the lower part of the section (Zone I), while temperate and warm broad-leaved
172 forest are relatively diverse and present throughout, but not particularly abundant in any zone. Steppe-desert pollen decreases
173 concurrently with a spike in tropical forest in Zone II, and then resurges to dominance in Zone III.



174

175 **Figure 2: Cumulative pollen summary diagram of the Ria Zhong (RZ) section in the Nangqian Basin, Yushu area, Tibet, with**
 176 **palynomorph percentages of the total pollen sum plotted on the x-axis, and zones and subzones based on CONISS ordinations.**
 177 **Productive horizons are indicated by a small trilete spore to the right of the simplified section log. The *Nitraria/Ephedra* (N/E) pollen**
 178 **ratio is plotted in purple, with a dashed line indicating the transition point between desert/semi-desert ecosystems (< 1) and steppe-**
 179 **desert (> 1).**

180

181 4.1 Stratigraphic zonation based on pollen

182 Based on results of two CONISS ordinations combined with the taxonomic and quantitative composition of the
 183 palynological assemblage (see Methods section; Fig. 2, Fig. S2 & S3), the succession was divided into three zones (I, II, III)
 184 of which Zone I was further divided into three subzones (a, b, c), all of which demonstrate unique vegetation dynamics
 185 within that zone. Important trends for each zone and subzone are described below. The zone boundaries are positioned at the



186 upper limit of the samples that mark each boundary. A complete overview of the raw counts, percentages and arithmetic
187 means are given in the supplementary information.

188

189





191 **Plate I: Light micrographs of selected pollen grains and spores from the Ria Zhong (RZ) section, Nangqian Basin. Scale bar –**
192 **10µm. 1-12. *Nitrariadites/Nitrariipollis*. 13-20. *Meliaceoidites*. 21-25. *Qinghaipollis*. 26-32. *Rhoipites*. 33-36. *Labitricolpites*. 37-45.**
193 ***Quercoidites*. 46. *Quercoidites minutus*. 47-51. *Rutaceoipollenites*. 52-54. *Momipites*. 55-58. *Fupingopollenites*. 59-61. *Ilexpollenites*.**
194 **62. *Aceripollenites*. 63-67. *Euphorbiacites*. 68-69. *Faguspollenites*. 70. *Retitricolporites*. 71. *Chenopodipollis*. 72. *Echitriporites* sp. 73.**
195 ***Sporopollis*. 74. *Caprifoliipites / Oleoidearumpollenites?*. 75-76. *Pterisisporites*. 77. Unidentified baculate spore. 78. *Liliacidites*. 79-80.**
196 ***Pterisisporites*. 81. *Taxodiacites*. 82-83. *Deltoidospora*. 84. *Lycopodiumsporites*. 85. *Spinizonocolpites*. 86-88. *Verrucosisporites*. 90.**
197 ***Lygodiumsporites*.**

198
199



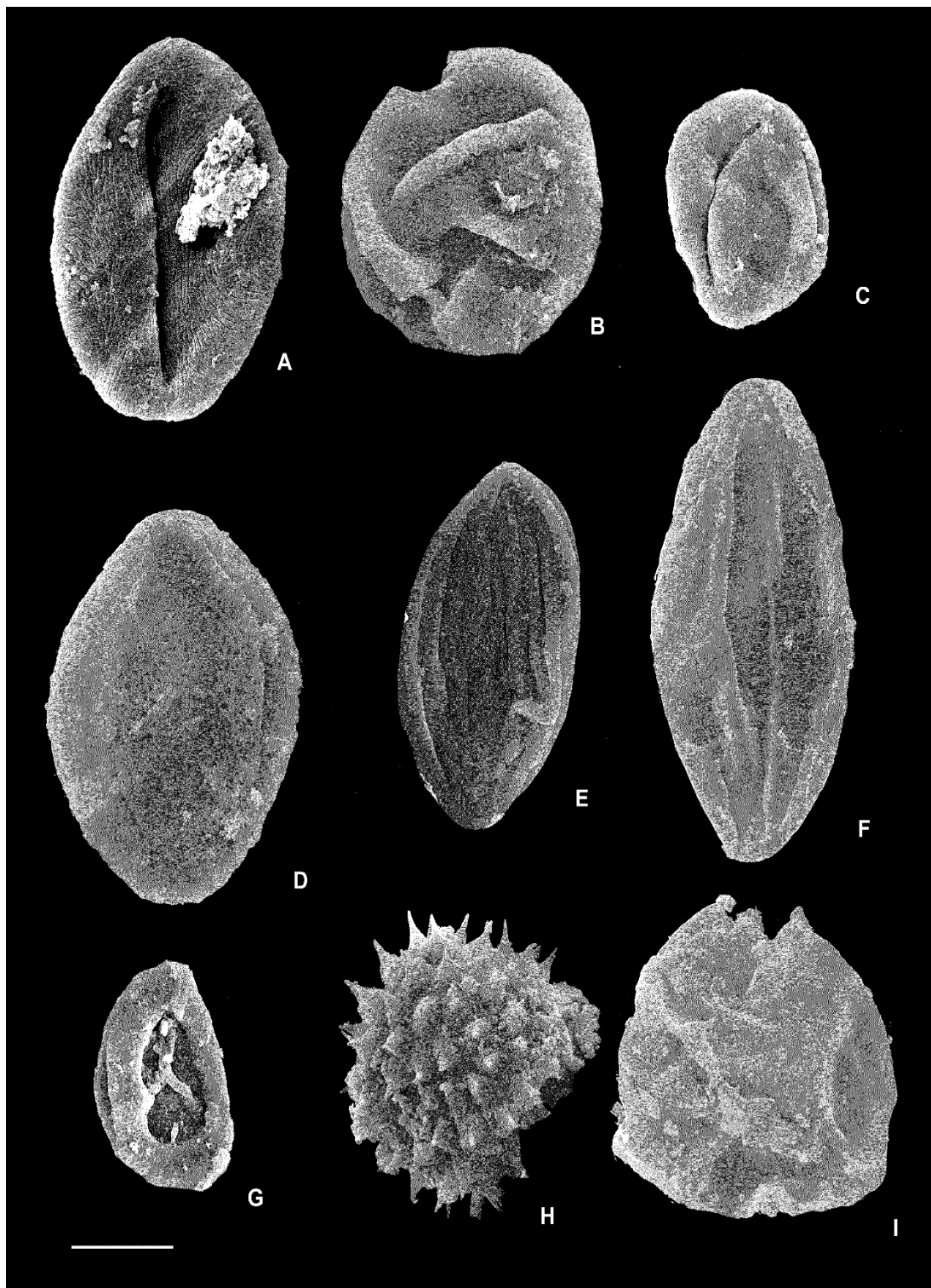
200

201 **Plate II: Light micrographs of ephedroid pollen from the Ria Zhong (RZ) section, Nangqian Basin. Scale bar – 10µm. A.**

202 ***Ephedripites (Distachyapites) cheganica*. B. *Ephedripites (Distachyapites) fusiformis*. C1-C4. *Ephedripites (Distachyapites)***



203 *megafusiformis*. **D1-D2.** *Ephedripites (Distachyapites) eocenipites*. **E1-E3.** *Ephedripites (Distachyapites) nanglingensis*. **F.** *Ephedripites*
204 *(Distachyapites) obesus*. **G.** *Ephedripites (Ephedripites) bernheidensis*. **I.** *Ephedripites (Ephedripites) sp. 2* (Han et al., 2016). **K.**
205 *Ephedripites (Ephedripites) sp. b.* **H.** *Ephedripites (Ephedripites) montanaensis*. **J.** *Ephedripites (Ephedripites) sp. a.* **L.**
206 *Steevesipollenites cf S. binodosus*. **M.** *Steevesipollenites jiangxiensis*.
207





209 **Plate III: Scanning Electron Microscope (SEM) photographs of selected fossil taxa in the Ria Zhong (RZ) section, Nangqian Basin.**
210 **Scale bar – 10µm. A, B, C. *Nitrariadites/Nitrariipollis*. D. *Retitricolporites*. E. *Ephedripites (Ephedripites) sp. 2* (Han et al., 2016). F.**
211 ***Ephedripites (Distachyapites) eocenipites*. G. *Pterisisporites*. H. Unidentified baculate spore. I. *Momipites*.**

212

213 **4.1.1 Zone I (17 samples, 251–155 m)**

214 Conifers in this zone are rare, represented only by *Taxodiacites* (Cupressaceae) and *Tsugaepollenites* (Pinaceae), and
215 never comprising more than 3%. The assemblage is dominated by steppe-desert taxa, which together comprise nearly 40%
216 and include numerous types of *Ephedripites* (Plate II), *Nitrariadites/Nitrariipollis*, and *Qinghaipollis*, together with more rare
217 xerophytic taxa such as *Chenopodipollis* and *Nanlingpollis*. The second most abundant group is the Pteridophytes (ferns),
218 which is also the most diverse of all the groups represented in the RZ section. Broad-leaved forest forms a minor component
219 of the pollen record, with warm forest being more abundant than temperate forest and represented primarily by
220 *Rutaceoipollenites*. Tropical forest pollen is rare, and includes *Spinizonocolpites* and *Fupingopollenites*. Some pollen types
221 have unresolved botanical affinities or affinities with multiple ecological groups, and these are grouped separately but do not
222 provide ecological information.

223 **Zone I** is divided into three subzones on the basis of abundance patterns among particular palynomorph taxa. Subzone
224 **Ia** (9 samples, 251–209 m) is unique in that *Ephedripites* (steppe-desert group), *Cupuliferoipollenites* (temperate forest), and
225 *Rutaceoipollenites* (warm forest) are more abundant than in other subzones of Zone I, while *Momipites* /
226 *Engelhardtioipollenites* (warm forest) is less abundant, and *Aceripollenites* + *Faguspollenites* (temperate forest) are very
227 rare compared to the remainder of Zone I. Of the entire section, *Caryophyllidites* (steppe-desert) only occurs in **Subzone Ib**
228 (3 samples, 203–187 m), which also records a spike of *Momipites/Engelhardtioipollenites* (warm forest). **Subzone Ic** (6
229 samples, 175.5–155 m) contains the greatest proportion of *Nanlingpollis* (steppe-desert) in the entire section, as well as
230 spikes of *Aceripollenites* + *Fraxinoipollenites* (temperate forest), while *Qinghaipollis* (steppe-desert) and ferns decrease in
231 this subzone.



232

233 **4.1.2 Zone II (2 samples, 110–107 m)**

234 No conifer pollen occurs in this zone, and on average, the steppe-desert taxa *Ephedripites* (gymnosperm),
235 *Nitrariadites/Nitrariipollis* and *Qinghapollis* (angiosperms) are far less abundant than in other parts of the section (average
236 9% in Zone II vs 38% (Zone I) and 32 % (Zone III)). However, a spike in the ancestral (old) *Ephedra* type is observed during
237 Zone II, which is not observed in the other zones or later in the Eocene (Yuan et al., 2017). Notably, tropical forest increases
238 markedly in this zone, comprising mostly *Fupingopollenites*, while temperate forest (*Aceripollenites*, cf. *Caprifoliipites*) and
239 warm forest (*Rutaceopollenites*) are also more prevalent. Pollen of unknown or multiple affinities is higher in this zone, and
240 reflected by spikes of *Labitricolpites* and *Rhoipites*.

241

242 **4.1.3 Zone III (3 samples, 107–16 m)**

243 Conifers in this zone are very rare, represented only by *Tsugaepollenites*. Steppe-desert taxa again dominate this zone,
244 with *Nitrariadites/Nitrariipollis* increasing steadily through the section. Temperate broad-leaved forest is now much more
245 common than warm or tropical forest pollen, while ferns are least common in this zone but still plentiful.

246

247 **5. Discussion**

248 **5.1 Age assignment**

249 Age constraints for the RZ section are provided by the K–Ar ages from shoshonitic lavas and felsic and porphyry
250 intrusions that are either interbedded with, or unconformably overlie, the lacustrine to alluvial Nangqian strata. Emplacement
251 ages across the Nangqian Basin vary between 32.04–36.5 Ma (Deng et al., 1999); 37.0 ± 0.2 Ma– 38.2 ± 0.1 Ma (Spurlin et
252 al., 2005); 37.1–37.8 Ma (Zhu et al., 2006); and 35.6 ± 0.3 – 39.5 ± 0.3 Ma (Xu et al., 2016). In the latter study, zircon U–Pb
253 age data were derived from felsic intrusions sampled at two localities in the Nangqian Basin (Boza and Nangqian). The
254 syenite porphyries from the Boza area (further south of the RZ section) show an emplacement age of 35.58 ± 0.33 Ma, while



255 the monzonite porphyries from the Nangqian area (just southeast of the RZ section) have older magmatic emplacement ages,
256 ranging from 39.5 ± 0.3 Ma to 37.4 ± 0.3 Ma. As this age range is broadly coeval with the age of the mafic volcanic rocks in
257 the Nangqian Basin (37.0–38.2 Ma; Spurlin et al., 2005) as well as the age range obtained by Zhu et al. (2006), here we
258 consider ~37–38 Ma to represent a minimum age for the RZ section. This is also congruent with palynological evidence for
259 the overall age of the sampled strata (Fig. 3), which is discussed in more detail below. The assemblage from the RZ section is
260 very similar to those from the Yang Ala section in the Nangqian Basin, dated as late Eocene (Yuan et al., 2017), the Eocene
261 Wuqia assemblage (site 98) from the west Tarim Basin (Wang et al., 1990a; 1990b), the late middle Eocene–late Eocene
262 assemblage from the upper Niubao Formation, Lunpola Basin (Song and Liu, 1982; Li et al., 2019), and the Bartonian part
263 of the palynological record in the Xining Basin (Dupont-Nivet et al., 2008; Hoorn et al., 2012; Han et al., 2016). Specifically,
264 the absence of *Classopollis*, *Exesipollenites*, and *Cycadopites* combined with the predominance of *Nitrariadites/Nitrariipollis*
265 and *Ephedripites* pollen, and the presence of the middle Eocene–Neogene genus *Fupinggopollenites* (Liu, 1985), indicates
266 that the RZ section cannot be older than Eocene (Fig. 3). It is also unlikely to be of latest Eocene age or younger due to the
267 lack of significant conifers that become more common approaching the Eocene–Oligocene Transition (Hoorn et al., 2012;
268 Page et al., 2019; Fig. 3). Specific ranges and abundance patterns of these and other key taxa within Eocene Tibetan basins
269 (Fig. 3; Fig. 4) enable the age of the section to be better constrained, which is explored in greater detail below.

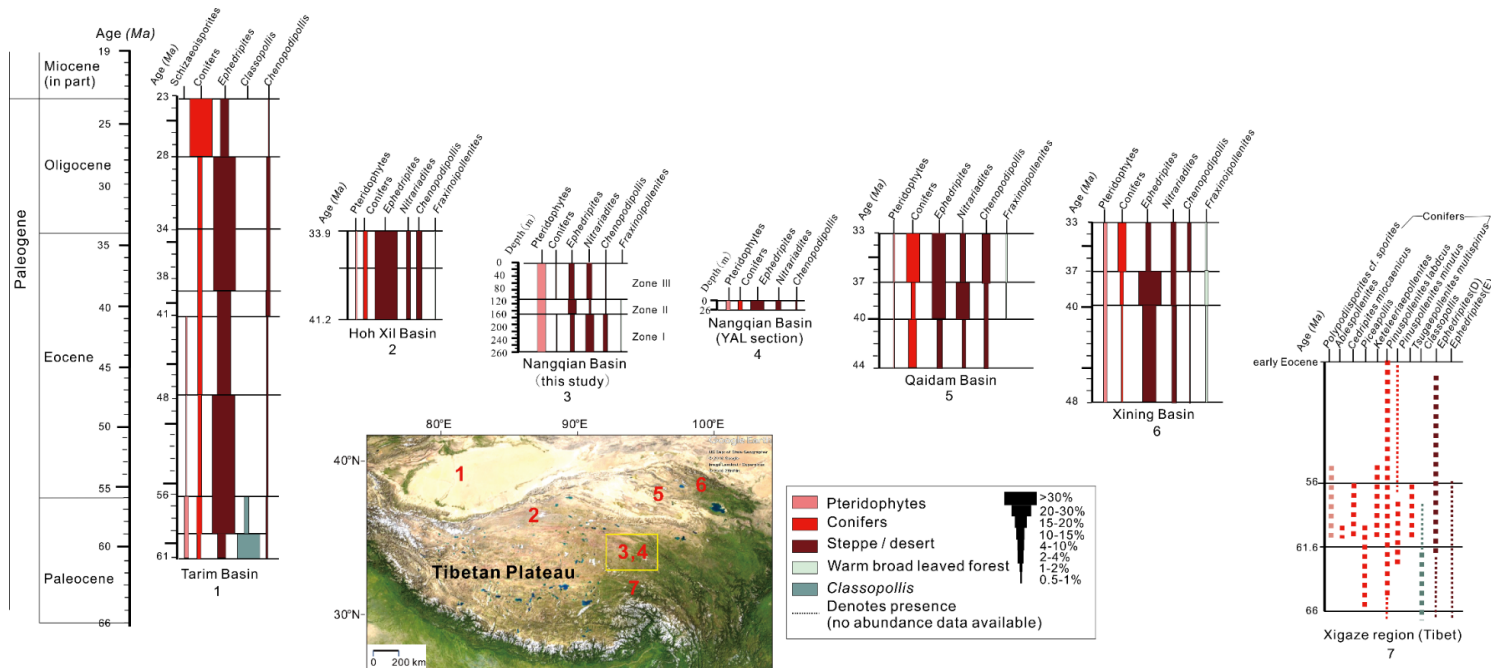
270 *Ephedra* is a gymnosperm shrub with the oldest macrofossils from the Early Cretaceous (Bolinder et al., 2016; Han et
271 al., 2016) but the genus is probably older, dating to the Triassic (Yang, 2002; Sun and Wang, 2005) or even the Permian
272 (Wang, 2004) based on the ephedroid pollen record. Its current distribution is limited primarily to arid and semiarid regions
273 of the world (Stanley et al., 2001), and the fossil pollen representative, *Ephedripites*, is widespread in Cenozoic evaporates,
274 indicating the xerophytic nature of this genus (Sun and Wang, 2005). In northern Tibet during the middle–late Eocene (after
275 38.8 Ma), *Ephedripites* comprised ca. 20–60% of the total pollen composition, with a predominance of the derived type,
276 *Ephedripites* subgen. *Distachyapites* (Han et al., 2016). Prior to this (ca. 41–38.8 Ma), the record comprised a mix of the
277 derived type, the ancestral type (*Ephedripites* subgen. *Ephedripites*), and another ephedroid genus, *Steevesipollenites* (Han et



278 al., 2016). A similar pattern is observed in the Nangqian Basin, with a spike of the ancestral type of *Ephedra* only recorded in
279 Zone II, and not observed in the rest of the RZ section or elsewhere in the Nangqian Basin (Yuan et al., 2017). This suggests
280 a correlation between Zone I of the Xining Basin with Zone II of the RZ section (Fig. 4).



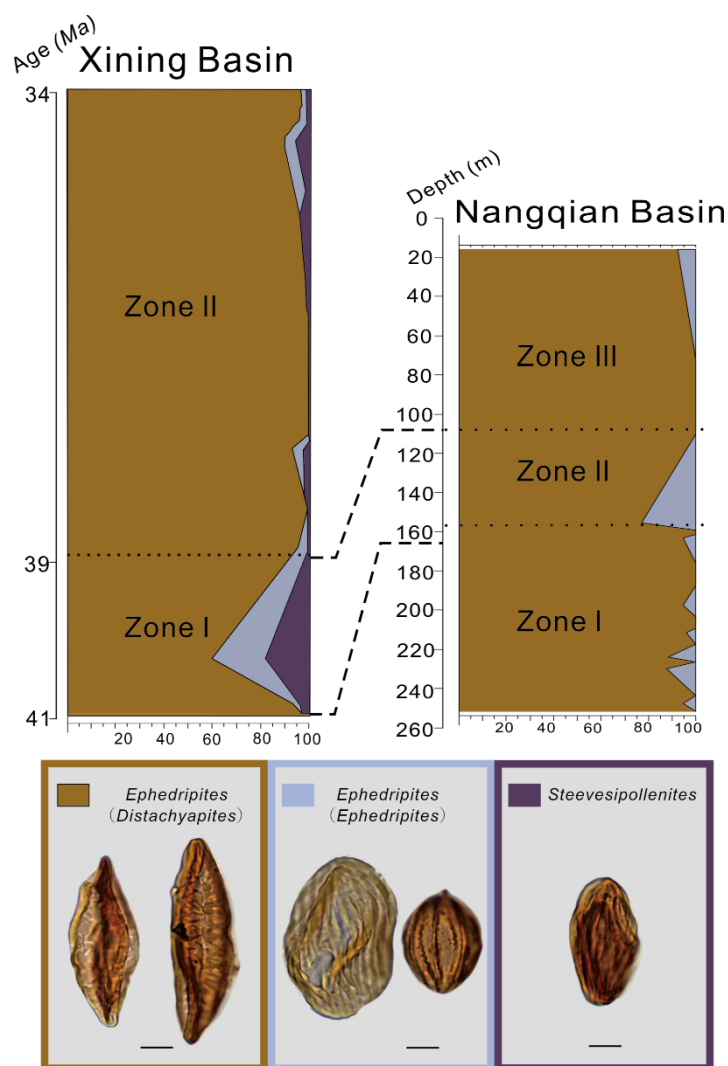
281



282 **Figure 3: Palynozonation of the Paleogene successions across the northern, central, and southern TP, with numbers under each section indicating the**
 283 **associated basin: 1. Tarim Basin (Wang et al., 1990a; 1990b); 2. Hoh Xil Basin (Miao et al., 2016); 3, 4. Nangqian Basin (this study; Yuan et al., 2017). 5.**
 284 **Qaidam Basin (Lu et al., 1985; Zhang et al., 2006; Miao et al., 2016); 6. Xining Basin (Wang et al., 1990a; 1990b; Hoorn et al., 2012); 7. Xigaze Basin (Li**
 285 **et al., 2008). Base map US Dept. of State Geographer, ©2018 Google, Image Landsat/Copernicus ©2018 ZENRIN.**



286



287

288 **Figure 4: Eocene ephedroid pollen composition in the Xining (northeastern TP) and Nangqian (east-central TP) basins, illustrating**
289 **the distributions of *Ephedripites* subgen. *Ephedripites*, *Ephedripites* subgen. *Distachyapites*, and *Steevesipollenites*.**

290 In addition to the proportions of the ancestral vs. derived type of *Ephedripites*, a significant spike in tropical forest
291 pollen at this time, combined with a large decrease in steppe-desert pollen, suggests that Zone II of the RZ section is likely
292 concurrent with the Middle Eocene Climatic Optimum (MECO; ~ 40 Ma). This event was a transient warming that preceded



293 rapid aridification in Central Asia (driven primarily by proto-Paratethys sea retreat; Kaya et al., 2019), indicated by
294 lithofacies and an increase in steppe-desert pollen records in northwestern China (Bosboom et al., 2014). Pollen records have
295 better constrained the drying event to occur between 40.7 and 39.9 Ma, after which vegetation became dominated by the
296 xerophytic and halophytic desert and steppe shrubs, *Ephedra* and *Nitraria*, along with a decrease in temperate broad-leaved
297 forest diversity (Meijer et al., submitted). These same patterns are observed in the shift from Zone II to Zone III in the RZ
298 section, Nangqian (Fig. 3). Although the spike of tropical forest pollen in Zone II of the RZ section is unusual, not being
299 observed elsewhere in the Nangqian Basin during the Eocene (this study; Yuan et al., 2017) or in the late Paleocene in
300 Nangqian (Barbolini et al. 2018: Barbolini, unpublished data), the upper zones of the RZ section yielded a low number of
301 samples, and the tropical forest spike is only present in one of these samples. Accordingly, further investigations should be
302 made in Nangqian and other parts of the Tibetan Plateau using independent age control to corroborate this finding. However,
303 it is unlikely that the pollen in Zone II represents reworking or contamination, as the palynomorphs from these samples were
304 not degraded or compressed to a greater degree than palynomorphs from the rest of the section, and of a similar colour and
305 appearance.

306 In northern Tibet, Pinaceae (conifers) abruptly increased in the palynological record at 36.55 Ma (Page et al., 2019),
307 which is not observed in the RZ section. The rare conifers in this latter assemblage are in accordance with the minimum
308 depositional age constraints of ~37–38 Ma from overlying volcanic rocks. In conjunction with the evidence described above
309 that links Zone II of the RZ section to the MECO, the age of the complete section is proposed to be late Lutetian–Bartonian
310 (Fig. 3; Fig. 4).

311

312 **5.2 Paleoclimate**

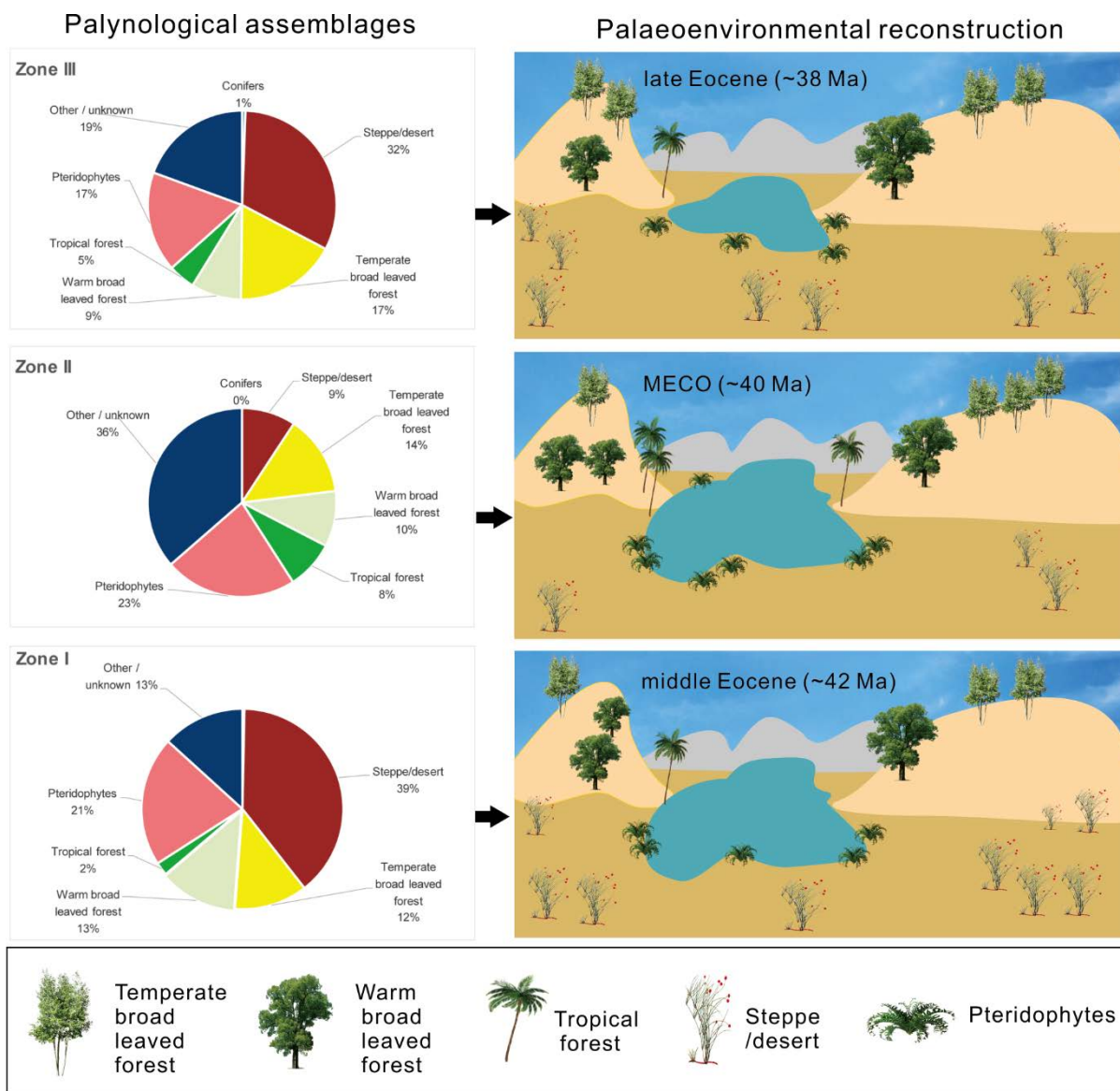
313 The RZ section records three distinct palaeofloras in east-central Tibet that evolved in response to changing climate in
314 the Eocene (Fig. 5). Before the MECO (Zone I), the climate was warm, and vegetation was characterised by steppe-desert
315 shrubs, diverse ferns, and a lesser component of temperate and warm broad-leaved forest. Interestingly, prominent vegetation



316 groups with very different moisture requirements existed within a limited distance of each another in the Nangqian area. A
317 very diverse and abundant pteridophyte community and conifers such as *Taxodiacites* and *Tsugaepollenites* would have
318 required higher humidity (Liu et al., 2012; Kotthoff et al., 2014), but the abundant halophytic and xerophytic steppe-desert
319 vegetation would likely only have been competitive in arid environments. The dominant plants belonging to these salt- and
320 drought- tolerant groups (*Nitraria* and *Ephedra*) grow today in Central Asian regions with MAP of 100mm or less, and are
321 also associated with arid palaeoenvironments through the Cenozoic (Sun & Wang, 2005). Although the conifers (produced
322 by cypress and *Tsuga*) could have been windblown from further distances, the coexistence of such diverse and abundant
323 pteridophytes and steppe-desert vegetation in the landscape, PFTs with opposing moisture requirements for competitiveness,
324 has not been observed in other Tibetan basins to date, and therefore seems not to reflect conventional spatial patterning of
325 less water-dependant vegetation growing upland. Rather, it may suggest an environment with strongly seasonal precipitation
326 that would favour lush vegetation growth for a restricted interval and alternately, xerophytic vegetation during the dry
327 season.

328

329



330

331 **Figure 5: Palaeoenvironmental reconstruction of the Nangqian area, illustrating the three distinct floral assemblages recovered from**
 332 **the RZ section. Vegetation in the late middle Eocene (Zone I) was dominated by steppe-desert plants, which decreased sharply over**
 333 **the Middle Eocene Climatic Optimum (MECO; Zone II) in conjunction with a spike in tropical forest. In the late Eocene the basin**
 334 **became drier and steppe-desert vegetation again dominated the landscape.**

335 Based on a comparison of existing palynofloral records with our new section, the northern regions of the plateau



336 (Tarim, Qaidam, Hoh Xil, and Xining basins) were already significantly more arid than the central TP prior to 40 Ma, having
337 hosted greater proportions of xerophytic plants (Fig. 3). Therefore, precipitation in the greater Nangqian region would have
338 been unlikely to derive from the westerlies, which served as the dominant moisture source northward of the central TP since
339 at least the early Eocene (Caves et al., 2015). This suggests that the central TP could have instead been influenced by a
340 southern monsoon system similar to the modern I-AM in the middle–late Eocene, although not to the degree experienced by
341 southern Tibet, which hosted greater proportions of forest and was likely more humid. However, it should be borne in mind
342 that rainfall seasonality is not always a proxy for the existence of monsoons; although leaf form is the preferred method for
343 detecting monsoons in deep time climates (Spicer et al., 2017), the absence of well-preserved fossil leaf assemblages from
344 the Nangqian Basin to date prevents this comparison.

345 Our results indicate that the MECO prompted a considerable change in the vegetation in east-central Tibet, encouraging
346 the temporary spread of (dry) forests while steppe-desert vegetation contracted (Zone II). Warming is reflected by an atypical
347 spike in tropical forest that coincides with a warm forest spike in northeastern Tibet (tropical forest is exceedingly rare in the
348 latter area during the middle–late Eocene), which demonstrates the regional influence of the MECO across (at least) the
349 northern and central parts of the TP. In order to estimate relative humidity in arid environments such as these, the
350 *Nitraria/Ephedra* (N/E) ratio can be used to distinguish between desert/semi-desert (< 1) and steppe-desert (> 1; Li et al.,
351 2005; Hoorn et al., 2012). Although both genera occupy arid environments today, *Ephedra* is currently distributed primarily
352 throughout deserts, semi-deserts and grasslands globally (Stanley et al., 2001), while *Nitraria* is a relatively more humid
353 steppe-desert taxon (Cour et al., 1999; Sun and Wang, 2005; Jiang and Ding, 2008; Li et al., 2009; Zhao and Herzschuh,
354 2009). In the RZ section, the proportion of temperate forest in relation to warm and tropical forest became much greater from
355 ca. 39 Ma (Fig. 2), indicating a cooler climate than prior to the MECO, which matches the cooling trend recorded by
356 clumped isotopes to the north (Page et al., 2019). Importantly, the N/E ratio in the RZ section is lowest immediately
357 following the MECO (Fig. 2) and persists for an extended period, indicating rapid, prolonged aridification, and an overall
358 expansion of steppe-desert vegetation is observed in Zone III, corresponding with patterns observed on the northeastern TP



359 (Bosboom et al., 2014; Meijer et al., submitted). Accordingly, our vegetation results have implications for understanding the
360 importance and extent of aridification across Central Asia after 40 Ma, which was primarily driven by proto-Paratethys Sea
361 regression (Kaya et al., 2019). The synchronous response of ecosystems to this event on both the northeastern and east-
362 central parts of the TP demonstrates that aridification across the Asian continental interior after 40 Ma was intense and
363 further-reaching than previously thought. Our findings show that after sea regression, westerly moisture supply carried from
364 the proto-Paratethys Sea was reduced as far as central Tibet. This provides further support for the argument that this sea was
365 a major source of moisture for the Asian interior, and thus a primary driver of Central Asian climate during the Eocene
366 (Bosboom et al., 2014; Bougeois et al., 2018; Kaya et al., 2019; Meijer et al., 2019).

367 Long-term aridification after the MECO exerted further influence on vegetational composition in east-central Tibet with
368 regards to the proportions of the ancestral vs. derived types of *Ephedripites*. In modern and Quaternary settings, this has been
369 developed as a ratio to distinguish between desert and steppe-desert environments, termed the *Ephedra fragilis*-type
370 s.l./*Ephedra distachya*-type (Ef/Ed) ratio (whereby *E. fragilis* represents the ancestral type and *E. distachya*, the derived
371 type). Tarasov et al. (1998) found the *E. fragilis*-type s.l. to be common in arid climates with mean temperatures of the
372 warmest month above 22°C. Herzschuh et al. (2004) applied the Ef/Ed ratio to Holocene pollen spectra from the Alashan
373 Plateau and tested its reliability with a regional modern pollen dataset, finding Ef/Ed ratios > 10 in most samples from desert
374 sites, and values < 5 in most samples from the sites with more favourable climates (e.g., forest-steppe, steppe, and alpine
375 meadow).

376 In the middle–late Eocene of Central Asia, the ancestral type of *Ephedripites* never comprises more than 25% of the
377 ephedroid pollen sum in northeastern Tibet while the derived type makes up at least 60% (Xining Basin; Han et al., 2016 and
378 Qaidam Basin; Zhu et al., 1985; Miao et al., 2013a; Jiuquan Basin; Miao et al., 2008), and this also appears true for
379 northwestern Tibet (Tarim Basin; Wang, et al., 1990b; Hoh Xil Basin; Miao et al., 2016) and east-central Tibet (Yuan et al.,
380 2017; this study). Therefore, Ef/Ed ratios > 10 (supposedly indicative of desert ecosystems) are never observed, despite the
381 N/E ratio indicating regular existence of deserts or semi-deserts in northern Tibet (Zhu et al., 1985; Hoorn et al., 2012; Miao



382 et al., 2016), and central Tibet (Yuan et al., 2017; this study) in the Eocene. Therefore, while pollen ratios appear to reflect
383 reliable functions of climate and landscape change for modern and Holocene settings (Li et al., 2010), our results identify
384 possible contradictions between the N/E and Ef/Ed pollen ratios. This indicates that further verification of these pollen ratios
385 in modern settings and across larger spatial scales is necessary for reliable palaeoenvironmental reconstructions in deep time.

386

387 **5.3 Elevational implications**

388 High-altitude conifers are rare in this particular record, although the high-elevation genus *Tsugaepollenites* (Fauquette
389 et al., 2006) is present. This could be driven by four possible factors: 1) taphonomy i.e., the assemblage has a high proportion
390 of autochthonous spores and pollen with little input from the peripheral mountains, 2) elevation of this region was relatively
391 low in the middle–late Eocene (< 3000m as proposed by Botsyun et al., 2019; also see Wei et al., 2016), 3) due to the
392 generally wetter climate in relation to the northeastern plateau basins, conifers are not competitive and surrounding
393 mountains are instead forested by temperate angiosperms, and 4) northern and central Tibet each record regional pollen
394 transported by different atmospheric circulation systems.

395 Regarding the first possibility, conifers are windblown and can be transported far distances (Lu et al., 2008; Ma et al.,
396 2008; Zhou et al., 2011); as the region already likely experienced a monsoonal climate (Spicer, 2017; Licht et al., 2014;
397 Caves et al., 2017; this study) we consider it unlikely that our assemblages record little to no regional vegetation. The second
398 factor, elevation history of the TP, is a controversial topic of discussion, and palynological evidence from the RZ section
399 does not provide strong support either for or against a relatively low middle–late Eocene palaeoaltitude in the region.
400 Although the upper part of the RZ section in the Nangqian Basin likely just pre-dates the high-elevation signal further to the
401 north from 37 Ma onwards (Dupont-Nivet et al., 2008; Hoorn et al., 2012; Page et al., 2019), an expanding body of data
402 indicates that a proto-Tibetan Highland with complex topography was already in place during the Paleogene (Xu et al., 2013;
403 Ding et al., 2014; Wang et al., 2014; Valdes et al., 2019). Furthermore, some of the broad-leaved angiosperms trees present in
404 the new Nangqian assemblage could have grown at maximum elevations of 3600–4000 m during the Eocene (*Ilex*, *Quercus*:



405 Song et al., 2010), and therefore their presence in lieu of abundant conifers is not in contradiction with an elevated
406 topography in parts of east-central Tibet at this time. This has significance for other Asian palynological studies that infer
407 regional palaeoaltitudes and uplift history of the TP based solely on palynological records from a single locality: a multi-
408 proxy approach is clearly necessary to address the complex history of TP uplift in future research.

409 Pollen data from the RZ assemblage supports climate (the third possibility) rather than altitude as a primary driving
410 factor of vegetational composition: locally wetter conditions in the east-central region of the TP (see Section 5.2) would
411 likely have promoted angiosperm tree growth over cold-temperate conifers that can withstand drought better, and utilise a
412 winter wet growing season unlike deciduous angiosperms (Dupont-Nivet et al., 2008; Hoorn et al., 2012; Page et al., 2019).
413 The last possibility is also supported, with the palynology of this study suggesting that central Tibet was influenced to a
414 limited degree by a southern monsoon in the middle–late Eocene, which could conceivably also have transported wind-
415 blown pollen from sub-tropical and warm temperate broad-leaved forests from the south (Su et al., 2018). In contrast, the
416 westerlies were the chief source of precipitation on the northern TP (see Section 5.2) and would have carried cold-temperate
417 conifer pollen from the mountains surrounding northeastern Tibet. Therefore, we propose that discrete local climatic
418 conditions and different regional atmospheric circulation systems were both primary driving factors of distinct floral
419 ecosystems in the northern and south-central TP during the middle–late Eocene.

420

421 6. Conclusions

422 On the basis of palynological assemblages, we conclude that the rocks of the RZ section (Nangqian Basin) are late
423 Lutetian–Bartonian (late middle–late Eocene) in age. They record a strongly seasonal steppe-desert ecosystem characterised
424 by *Ephedra* and *Nitraria* shrubs, diverse ferns and an underlying component of broad-leaved forests. The climate became
425 significantly warmer over the MECO, encouraging forest growth and a proliferation of the thermophilic ancestral *Ephedra*
426 type, but rapidly aridified thereafter due primarily to regression of the proto-Paratethys Sea. This is in conjunction with
427 observed environmental shifts in northeastern Tibet, and provides further support for widespread Asian aridification after 40



428 Ma. A new palynozonation better constrains the biostratigraphy of Paleogene successions across the northern, central, and
429 southern TP, and also illustrates local ecological variability during the Eocene. This highlights the ongoing challenge of
430 integrating various deep time records for the purpose of reconstructing palaeoelevation, and suggests that a multiproxy
431 approach is vital for unravelling the complex uplift history of the TP.

432

433 **Author contribution**

434 Q.Y., V.V., F.S.S., D.L.G., H.C.W. and Q.S.F. conceptualized the study. Q.Y., F.S.S., H.C.W., Z.J.Q., Y.S.D. and J.J.S.
435 carried out fieldwork. Q.Y., N.B., V.V. and C.R. collected and analysed the data. Q.Y. wrote the first draft and N.B., V.V., and
436 C.R. participated in review and editing of the final draft.

437

438 **Competing interests**

439 The authors declare that they have no conflict of interest.

440

441 **Acknowledgments**

442 We thank Dr. Fuyuan An (Qinghai Normal University), Dr. Shuang Lü (University of Tübingen), and Aijun Sun
443 (University of Chinese Academy of Sciences) for assistance in the fieldwork, and Prof. Yunfa Miao (Chinese Academy of
444 Sciences) for helpful discussions on the systematic palynology. This work was supported by the National Natural Science
445 Foundation of China (grant 41302024 to Q.Y.); The Youth Guiding Fund of Qinghai Institute of Salt Lakes, CAS (grant
446 Y360391053 to Q.Y.); The Second Tibetan Plateau Scientific Expedition and Research Program (STEP) CAS (grant 2019
447 QZKK0805 to Q.Y.), and the Swedish Research Council (VR) grants 2015-4264 to V.V. and 2017-03985 to C.R. Funding
448 sources had no involvement in study design.

449

450 **Data availability**



451 The authors declare that all data supporting the findings of this study are available in the supplementary information or
452 published in a data repository at the following DOI: 10.17632/xvp68wsd2p.3 (Yuan and Barbolini, 2020).

453

454 **Supplementary information**

455 Supplementary information is available for this paper (Fig. S1, S2, S3).

456

457 **References**

- 458 Abels, H. A., Dupont - Nivet, G., Xiao, G., Bosboom, R., and Krijgsman, W.: Step - wise change of Asian interior climate
459 preceding the Eocene - Oligocene Transition (EOT), *Palaeogeogr. Palaeoclimatol. Palaeoecol.*, 299, 399–412, 2011.
- 460 Aitchison, J.C., and Davis, A.M.: When did the India–Asia collision really happen? *Gondwana. Res.*, 4, 560–561, 2001.
- 461 Aitchison, J.C., Xia, X.P., Baxter, A.T., and Ali, J.R.: Detrital zircon U-Pb ages along the Yarlung-Tsangpo suture zone,
462 Tibet: implications for oblique convergence and collision between India and Asia, *Gondwana. Res.*, 20, 691–709, 2011.
- 463 Barbolini, N., Dupont-Nivet, G., Meijer, N., Jardine, P.E., Rohrmann, A., and Hoorn, C.: Multiple palaeoecological proxies
464 constrain the interplay between Tibetan Plateau growth, the proto-monsoons and floral dispersal during the early India-
465 Asia collision. European Palaeobotany and Palynology Conference, 12–17 August 2018, Dublin, Ireland, 2018.
- 466 Baumann, F., He, J.S., Scheidt, K., Kühn, P., and Scholten, T.: Pedogenesis, permafrost, and soil moisture as controlling
467 factors for soil nitrogen and carbon contents across the Tibetan Plateau, *Glob. Change Biol.*, 15, 3001–3017, 2009.
- 468 Bolinder, K., Norbäck Ivarsson, L., Humphreys, A.M., Ickert-Bond, S.M., Han, F., Hoorn, C., and Rydin, C.: Pollen
469 morphology of *Ephedra* (Gnetales) and its evolutionary implications, *Grana*, 55, 24–51, 2016.
- 470 Bosboom, R.E., Dupont-Nivet, G., Houben, A.J.P., Brinkhuis, H., Villa, G., Mandic, O., Stoica, M., Zachariasse, W.J., Guo,
471 Z.J, Li, C.X, and Krijgsman, W.: Late Eocene sea retreat from the Tarim Basin (west China) and concomitant Asian
472 paleoenvironmental change, *Palaeogeogr. Palaeoclimatol. Palaeoecol.*, 299, 385–398, 2011.
- 473 Bosboom, R.E., Abels, H.A., Hoorn, G., Van den berg, B.C.J., Guo, Z.J., and Dupont-Nivet, G.: Aridification in continental
474 Asia after the Middle Eocene Climatic Optimum (MECO), *Earth Planet. Sci. Lett.*, 389, 34–42, 2014.



- 475 Botsyun, S., Sepulchre, P., Donnadieu, Y., Risi, C., Licht, A., and Caves Rügenstein, J.: Revised paleoaltimetry data show
476 low Tibetan Plateau elevation during the Eocene, *Science*, 363, eaaq1436, 2019.
- 477 Bougeois, L., Dupont-Nivet, G., De Raféllis, M., Tindall, J., Proust, J.N., Reichart, G.J., Nooijer, L., Guo, Z.J., and Ormukov,
478 C.: Asian monsoons and aridification response to Paleogene sea retreat and Neogene westerly shielding indicated by
479 seasonality in Paratethys oysters, *Earth Planet. Sci. Lett.*, 485, 99–110, 2018.
- 480 Cai, M.T., Fang, X.M., Wu, F.L., Miao, Y.F., and Appel, E.: Pliocene–Pleistocene stepwise drying of Central Asia: evidence
481 from paleo-magnetism and sporopollen record of the deep borehole SG-3 in the western Qaidam Basin, NE Tibetan
482 Plateau, *Global. Planet. Change*, 94–95, 72–81, 2012.
- 483 Caves, J.K.: The Cenozoic climate and tectonic history of Asia. Thesis. (PhD Thesis). Stanford University, California, 400
484 pp. 2016.
- 485 Caves, J.K., Sjostrom, D.J., Mix, H.T., Winnick, M.J., and Chamberlain, C.P.: Aridification of Central Asia and uplift of the
486 Altai and Hangay Mountains, Mongolia: Stable isotope evidence, *Am. J. Sci.*, 314, 1171–1201, 2014.
- 487 Caves, J.K., Winnick, M.J., Graham, S.A., Sjostrom, D.J., Mulch, A., and Chamberlain, C.P.: Role of the westerlies in
488 Central Asia climate over the Cenozoic, *Earth Planet. Sci. Lett.*, 428, 33–43, 2015.
- 489 Cour, P., Zheng, Z., Duzer, D., Calleja, M., and Yao, Z.: Vegetational and climatic significance of modern pollen rain in
490 northwestern Tibet, *Rev. Palaeobot. Palynol.*, 104, 183–204, 1999.
- 491 DeConto, R.M., and Pollard, D.: Rapid Cenozoic glaciation of Antarctica induced by declining atmospheric CO₂, *Nature*,
492 421, 245–249, 2003.
- 493 Deng, W., Sun, H., and Zhang, Y.: Cenozoic K–Ar ages of volcanic rocks in the Nangqian Basin, Qinghai, *Chinese Sci.*
494 *Bull.*, 44, 2554–2558, 1999. (in Chinese with English abstract).
- 495 Ding, L., Xu, Q., Yue, Y.H., Wang, H.Q., Cai, F.I., and Li, S.: The Andean-type Gangdese Mountains: paleoelevation record
496 from the Paleocene-Eocene Linzhou Basin, *Earth Planet. Sci. Lett.*, 392, 250–264, 2014.
- 497 Dupont-Nivet, G., Keijsman, W., Langereis, C.G., Abels, H.A., Dai, S., and Fang, X.M.: Tibetan plateau aridification linked



- 498 to global cooling at the Eocene-Oligocene transition, *Nature*, 445, 635–638, 2007.
- 499 Dupont-Nivet, G., Hoorn, C., and Konert, M.: Tibetan uplift prior to the Eocene–Oligocene climate transition: evidence from
500 pollen analysis of the Xining Basin, *Geology*, 36, 987–990, 2008.
- 501 Fauquette, S., Suc, J.P., Bertini, A., Popescu, S.M., Warny, S., Taoufiq, N.B., Villa, M.J.P., Chikhi, H., Feddi, N., Subally, D.,
502 and Clauzon, G.: How much did climate force the Messinian salinity crisis? Quantified climatic conditions from pollen
503 records in the Mediterranean region, *Palaeogeogr. Palaeoclimatol. Palaeoecol.*, 238, 281–301, 2006.
- 504 Grimm, E.C.: CONISS: a FORTRAN 77 program for stratigraphically constrained cluster analysis by the method of
505 incremental sum of squares. *Comput Geosci UK.*, 13(1), 13–35, 1987.
- 506 Grimm, E.C.: TILIA v2. 0. b. 4 and TGView v2. 0 (computer software), Illinois State Museum, Research and Collections
507 Center, Springfield, IL, USA, 1991. <https://www.tiliait.com/>
- 508 Gupta, A. K., Singh, R. K., Joseph, S., and Thomas, E.: Indian Ocean high-productivity event (10–8 Ma): Linked to global
509 cooling or to the initiation of the Indian monsoons? *Geology*, 32, 753–756, 2004.
- 510 Han, F., Rydin, C., Bolinder, K., Dupont-Nivet, G., Abels, H.A., Koutsodendris, A., Zhang, K., and Hoorn, C.: Steppe
511 development on the Northern Tibetan Plateau inferred from Paleogene ephedroid pollen, *Grana*, 55, 71–100, 2016.
- 512 Han, J.L., Han, F.Q., Hussain, S.A., Liu, W.Y., Nian, X.Q., and Mao, Q.F.: Origin of Boron and Brine Evolution in Saline
513 Springs in the Nangqen Basin, Southern Tibetan Plateau, *Geofluids*, 2018, 1–12, 2018.
- 514 Herb, C., Koutsodendris, A., Zhang, W.L., Appel, E., Fang, X.M., Voigt, S., and Pross, J.: Late Plio-Pleistocene humidity
515 fluctuations in the western Qaidam Basin (NE Tibetan Plateau) revealed by an integrated magnetic-palynological record
516 from lacustrine sediments, *Quat. Res.*, 84, 457–466, 2015.
- 517 Herzschuh, U., and Liu, X.Q.: Vegetation evolution in arid China during Marine Isotope Stages 3 and 2 (~ 65–11 Ka).
518 Developments in Quaternary, *Science*, 9, 41–49, 2007.
- 519 Herzschuh, U., Tarasov, P., Wünnemann, B., and Hartmann, K., Holocene vegetation and climate of the Alashan Plateau NW
520 China, reconstructed from pollen data, *Palaeogeogr. Palaeoclimatol. Palaeoecol.*, 211, 1–17, 2004.



- 521 Hoorn, C., Straathof, J., Abels, H.A., Xu, Y.D., Utescher, T., and Dupont-Nivet, G.: A late Eocene palynological record of
522 climate change and the Tibetan Plateau uplift (Xining Basin, China), *Palaeogeogr. Palaeoclimatol. Palaeoecol.*, 344, 16–
523 38, 2012.
- 524 Horton, B.K., Yin, A., Spurlin, M.S., Zhou, J., and Wang, J.: Paleocene–Eocene syncontractional sedimentation in narrow,
525 lacustrine-dominated basins of east-central Tibet, *Geol. Soc. Am. Bull.*, 114, 771–786, 2002.
- 526 Hou, Z., Hongwen, M., Zaw, K., Yuquan, Z., Mingjie, W., Zeng, W., Guitang, P., and Renli, T.: The Himalayan Yulong
527 porphyry copper belt: product of large-scale strike-slip faulting in eastern Tibet, *Econ. Geol.*, 98, 125–145, 2003.
- 528 Hu, X.M., Garzanti, E., Wang, J.G., Huang, W.T., An, W., and Webb, A.: The timing of India-Asia collision onset- Facts,
529 theories, controversies, *Earth-Sci. Rev.*, 160, 264–299, 2016.
- 530 Ji, L.M., Meng, F.W., Yan, K., and Song, Z.G.: The dinoflagellate cyst *Subtilisphaera* from the Eocene of the Qaidam Basin,
531 northwest China, and its implications for hydrocarbon exploration, *Rev. Palaeobot. Palynol.*, 167, 40–50, 2011.
- 532 Jiang, H., and Ding, Z.: A 20 Ma pollen record of East-Asian summer monsoon evolution from Guyuan, Ningxia, China,
533 *Palaeogeogr. Palaeoclimatol. Palaeoecol.*, 265, 30–38, 2008.
- 534 Jiang, Y.B., Guo, F.S., Hou, Z.Q., Yang, T.N., Liu, Y.X., Yang, Q.K., and Du, H.F.: Sedimentary features and evolution of the
535 Nangqian Paleogene basin in northeastern Qinghai-Tibet Plateau, *Acta petrol. Et. Miner.*, 30, 391–400, 2011. (in
536 Chinese with English abstract).
- 537 Jin, C., Liu, Q., Liang, W., Roberts, A.P., Sun, J., Hu, P., Zhao, X., Su, Y., Jiang, Z., Liu, Z. and Duan, Z.:
538 Magnetostratigraphy of the Fenghuoshan Group in the Hoh Xil Basin and its tectonic implications for India–Eurasia
539 collision and Tibetan Plateau deformation, *Earth Planet. Sci. Lett.*, 486, 41–53, 2018.
- 540 Kaya, M.Y., Dupont-Nivet, G., Proust, J.-N., Roperch, P., Bougeois, L., Meijer, N., Frieling, J., Fioroni, C., Altiner, S.Ö.,
541 Vardar, E., Barbolini, N., Stoica, M., Aminov, J., Mamtimin, M., and Guo, Z.: Paleogene evolution and demise of the
542 proto-Paratethys Sea in Central Asia (Tarim and Tajik basins): role of intensified tectonic activity at ~41 Ma, *Basin
543 Res.*, 31, 461–486, 2019.



- 544 Kotthoff, U., Greenwood, D.R., McCarthy, F.M.G., Müller-Navarra, K., Prader, S., and Hesselbo, S.P.: Late
545 Eocene to middle Miocene (33 to 13 million years ago) vegetation and climate development on the North
546 American Atlantic Coastal Plain (IODP Expedition 313, Site M0027), *Clim. Past.*, 10, 1523–1539, 2014.
- 547 Li, F., Sun, J., Zhao, Y., Guo, X., Zhao, W. and Zhang, K.: Ecological significance of common pollen ratios: A review. *Front.*
548 *Earth Sci. Chin.*, 4(3), 253–258, 2010.
- 549 Li, J.G., Batten, D.J., and Zhang, Y.Y.: Palynological indications of environmental changes during the Late Cretaceous–
550 Eocene on the southern continental margin of Laurasia, Xizang (Tibet), *Palaeogeogr. Palaeoclimatol. Palaeoecol.*, 265,
551 78–86, 2008.
- 552 Li, J.G., Wu, Y.X., Batten, D.J., and Lin, M.Q.: Vegetation and climate of the central and northern Qinghai–Xizang plateau,
553 *J. Asian. Earth. Sci.*, 175, 34–38, 2019.
- 554 Li, S.Y., Currie, B.S., Rowley, D.B., and Ingalls, M.: Cenozoic paleoaltimetry of the SE margin of the Tibetan Plateau:
555 Constraints on the tectonic evolution of the region, *Earth Planet. Sci. Lett.*, 432, 415–424, 2015.
- 556 Li, Y., Xu, Q., Zhao, Y., Yang, X., Xiao, J., Chen, H., and Lü, X.: Pollen indication to source plants in the eastern desert of
557 China, *Chinese. Sci. Bull.*, 50 (15), 1632–1641, 2005.
- 558 Li, Y., Wang, N., Morrill, C., Cheng, H., Long, H., and Zhao, Q.: Environmental change implied by the relationship between
559 pollen assemblages and grain-size in N.W. Chinese lake sediments since the Late Glacial, *Rev. Palaeobot. Palynol.*, 154,
560 54–64, 2009.
- 561 Li, X., Zhang, R., Zhang, Z. and Yan, Q.: What enhanced the aridity in Eocene Asian inland: Global cooling or early Tibetan
562 Plateau uplift? *Palaeogeogr. Palaeoclimatol. Palaeoecol.*, 510, 6–14, 2018.
- 563 Li, X.M., Peng, T.J., Ma, Z.H., Li, M., Feng, Z.T., Guo, B.H., Yu, H., Ye, X.Y., Hui, Z.C., Song, C.H., and Li,
564 J.J.: Late Miocene–Pliocene climate evolution recorded by the red clay cover on the Xiaoshuizi planation
565 surface, NE Tibetan Plateau, *Clim. Past.*, 15, 405–421, 2019.
- 566 Licht, A., Cappelle, M.V., Ables, H.A., Ladant, J.B., Trabucho-Alexandre, J., France-Lanord, C., Donnadieu, Y.,



- 567 Vandenberghe, J., Rigaudier, T., Lecuyer, C., Terry Jr, D., Adriaens, R., Boura, A., Guo, Z., Soe, A.N., Quade, J.,
568 Dupont-Nivet, G., Jaeger, J.J.: Asian monsoons in a late Eocene greenhouse world, *Nature*, 513, 501–506, 2014.
- 569 Liu, G.W., *Fupingopollenites* gen. nov. and its distribution, *Acta. Palaeontol. Sin.*, 24, 64–70, 1985. (in Chinese with English
570 abstract).
- 571 Liu, J., Li, J.J., Song, C.H., Yu, H., Peng, T.J., Hui, Z.C., and Ye, X.Y.: Palynological evidence for late Miocene
572 stepwise aridification on the northeastern Tibetan Plateau, *Clim. Past*, 12, 1473–1484, 2016.
- 573 Liu, Y., Liu, H., Theye, T. and Massonne, H.J.: Evidence for oceanic subduction at the NE Gondwana margin during Permo-
574 Triassic times, *Terra Nova*, 21(3), 195–202, 2009.
- 575 Liu, Z., Zhao, X., Wang, C.S., and Liu, H.Y.: Magnetostratigraphy of Tertiary sediments from the Hoh Xil Basin:
576 implications for the Cenozoic tectonic history of the Tibetan Plateau, *J. Asian. Earth. Sci.*, 154, 233–252, 2003.
- 577 Liu, Z.Q.: Geologic map of the Qinghai-Xizang Plateau and its neighboring regions: Beijing, Chengdu Institute of Geology
578 and Mineral Resources, Geologic Publishing House, scale 1:1 500 000. 1988.
- 579 Lu, H., Wu, N., Yang, X., Shen, C., Zhu, L., Wang, L., Li, Q., Xu, D., Tong, G., and Sun, X.: Spatial patterns of *Abies* and
580 *Picea* surface pollen distribution along the elevation gradient in the Qinghai–Tibetan Plateau and Xinjiang, China,
581 *Boreas*, 37, 254–262, 2008.
- 582 Lu, J.F., Song, B.W., Chen, R.M., Zhang, J.Y., and Ye, H.: Palynological assemblage of Eocene–Oligocene pollen and their
583 biostratigraphic correlation in Dahonggou, Daqaidam Regions, Qaidam Basin, *Earth Sci. J. China University of*
584 *Geosciences*, 35, 839–848, 2010. (in Chinese, with English abstract).
- 585 Ma, Y., Liu, K., Feng, Z., Sang, Y., Wang, W., and Sun, A.: A survey of modern pollen and vegetation along a south–north
586 transect in Mongolia, *J. Biogeogr.*, 35, 1512–1532, 2008.
- 587 Mao, Y.B.: Tectonic evolvement Coal accumulation in Zaduo-Nangqian area of Qinghai Province, *J. Earth Sci. Environ.*, 32,
588 225–233, 2010. (in Chinese)
- 589 Meijer, N., Dupont-Nivet, G., Abels, H.A., Kaya, M.Y., Licht, A., Xiao, M.M., Zhang, Y., Roperch, P., Poujol, M., Lai, Z.P.,



- 590 and Guo, Z.J.: Central Asian moisture modulated by proto-Paratethys Sea incursions since the early Eocene, *Earth*
591 *Planet. Sci. Lett.*, 510, 73–84, 2019.
- 592 Miao, Y.F.: Cenozoic Pollen Records in the Xining Basin and Its Significance for the Palaeoclimate Change. Postdoctoral
593 Report. Institute of Tibetan Plateau Research, Chinese Academy of Sciences, Beijing, 95 pp, 2010. (in Chinese with
594 English abstract).
- 595 Miao, Y.F., Fang, X.M., Song, Z.C., Wu, F.L., Han, W.X., Dai, S. and Song, C.H.: Late Eocene pollen records and
596 paleoenvironmental changes in northern Tibetan Plateau, *Sci. China. Earth. Sci.*, 51, 1089–1098, 2008.
- 597 Miao, Y.F., Fang, X.M., Herrmann, M., Wu, F.L., Zhang, Y.Z., and Liu, D.L.: Miocene pollen record of KC-1 core in the
598 Qaidam Basin, NE Tibetan Plateau and implications for evolution of the East Asian monsoon, *Palaeogeogr.*
599 *Palaeoclimatol. Palaeoecol.*, 299, 30–38, 2011.
- 600 Miao, Y.F., Herrmann, M., Wu, F.L., Yan, X.L., and Yang, S.L.: What controlled Mid-Late Miocene long-term aridification in
601 Central Asia? Global cooling or Tibetan Plateau uplift: a review, *Earth. Sci. Rev.*, 112, 155–172, 2012.
- 602 Miao, Y.F., Fang, X.M., Wu, F.L., and Cai, M.T.: Late Cenozoic continuous aridification in the western Qaidam Basin:
603 evidence from sporopollen records, *Clim. Past.* 9, 1863–1877, 2013a.
- 604 Miao, Y.F., Fang, X.M., Song, C.H., Yan, X.L., Xu, L., and Chen, C.F.: Pollen and fossil wood’s linkage with Mi-1
605 Glaciation in northeastern Tibetan Plateau, China, *Palaeoworld*, 22, 101–108, 2013b.
- 606 Miao, Y.F., Wu, F.L., Chang, H., Fang, X.M., Deng, T., Sun, X.M., and Jin, C.S.: A Late Eocene palynological record from
607 the Hoh Xil Basin, Northern Tibetan Plateau, and its implications for stratigraphic age, paleoclimate and paleoelevation,
608 *Gondwana. Res.*, 31, 241–252, 2016.
- 609 Molnar, P.: Late Cenozoic increase in accumulation rates of terrestrial sediments: How might climate change have affected
610 erosion rates? *Annu. Rev. Earth Planet. Sci.*, 32, 67–89, 2004.
- 611 Molnar, P., and Tapponnier, P.: Effects of a Continental Collision, *Science*, 189, 419–426, 1975.
- 612 Molnar, P., Boos, W.R., and Battisti, D.S.: Orographic controls on climate and paleoclimate of Asia: thermal and mechanical



- 613 roles for the Tibetan Plateau, *Annu. Rev. Earth Planet. Sci.*, 38, 77–102, 2010.
- 614 Mulch, A., and Chamberlain, C.P.: Stable isotope paleoaltimetry in orogenic belts — the silicate record in surface and crustal
615 geological archives, *Reviews in Mineralogy and Geochemistry*, 66, 89–118, 2007.
- 616 Paeth, H., Steger, C., Li, J.M., Mutz, S.G. and Ehlers, T.A.: Comparison of Cenozoic surface uplift and glacial-
617 interglacial cycles on Himalaya-Tibet paleo-climate: Insights from a regional climate model, *Global*
618 *Planet. Change*, 177, 10–26, 2019.
- 619 Page, M., Licht, A., and Dupont-Nivet, G.: Synchronous cooling and decline in monsoonal rainfall in northeastern Tibet
620 during the fall into the Oligocene icehouse, *Geology*, 47(3), 203–206, 2019.
- 621 Pagani, M., Hubei, M., Liu, Z.H., Bohaty, S.M., Henderikes, J., Sijp, W., Krishnan, S., and DeConto, R.M.: The role of
622 carbon dioxide during the onset of Antarctic glaciation, *Science*, 334, 1261–1264, 2011.
- 623 Qinghai BGMR, (Qinghai Bureau of Geology and Mineral Resources), Geologic map of the Nangqian region, with geologic
624 report: unpublished, 198 pp., scale 1:200 000. 1983a.
- 625 Qinghai BGMR, (Qinghai Bureau of Geology and Mineral Resources), Geologic map of the Shanglaxiu region, with
626 geologic report: unpublished, 220 pp., scale 1:200 000. 1983b.
- 627 Qinghai BGMR, (Qinghai Bureau of Geology and Mineral Resources), Regional Geology of Qinghai Province: Beijing,
628 Geological Publishing House, 662 pp. 1991.
- 629 Rowley, D.B., and Currie, B.S.: Palaeo-altimetry of the late Eocene to Miocene Lunpola basin, central Tibet, *Nature*, 439,
630 677–681, 2006.
- 631 Shen, H., and Poulsen, C.J.: Precipitation $\delta^{18}\text{O}$ on the Himalaya–Tibet orogeny and its relationship to surface
632 elevation, *Clim. Past*, 15, 169–187, 2019.
- 633 Song, X.Y., Spicer, R.A., Yan, J., Yao, Y.F., and Li, C.S.: Pollen evidence for an Eocene to Miocene elevation of central
634 southern Tibet predating the rise of the High Himalaya, *Palaeogeogr. Palaeoclimatol. Palaeoecol.*, 297, 159–168, 2010.
- 635 Song, Z.C., and Liu, G.W.: Early Tertiary palynoflora and its significance of palaeogeography from northern and eastern



- 636 Xizang. In: Integrative Scientific Expedition Team to the Qinghai–Xizang plateau, Academia Sinica (ed.),
637 Palaeontology of Xizang. Book V. Science Press, Beijing, 183–201, 1982. (in Chinese with English abstract).
- 638 Spicer, R.A.: Tibet, the Himalaya, Asian monsoons and biodiversity in what ways are they related? *Plant Diversity*, 39, 233–
639 244, 2017.
- 640 Spurlin, M.S., Yin, A., Horton, B.K., Zhou, J., and Wang, J.: Structural evolution of the Yushu–Nangqian region and its
641 relationship to syncollisional igneous activity, east-central Tibet, *Geol. Soc. Am. Bull.*, 117, 1293–1317, 2005.
- 642 Stanley, C., Charlet, D.A., Freitag, H., Maier-Stolte, M., and Starratt, A.N.: New observations on the secondary chemistry of
643 world *Ephedra* (Ephedraceae), *Am. J. Bot.*, 88, 1199–1208, 2001.
- 644 Su, T., Spicer, R.A., Li, S.H., Huang, J., Sherlock, S., Huang, Y.J., Li, S.F., Wang, Li., Jia, L.B., Deng, W.Y.D., Liu, J., Deng,
645 C.L., Zhang, S.T., Valdes, P.J., and Zhou, Z.K.: Uplift, climate and biotic changes at the Eocene-Oligocene transition
646 in south-eastern Tibet, *Natl. Sci. Rev.*, 6(3), 495–504, 2018.
- 647 Su, T., Farnsworth, A., Spicer, R.A., Huang, J., Wu, F.X., Liu, J., Li, S.F., Xing, Y.W., Huang, Y.J., Deng, W.Y.D., Tang, H.,
648 Xu, C.L., Zhao, F., Srivastava, G., Valdes, P.J., Deng, T., and Zhou, Z.K.: No high Tibetan Plateau until the Neogene,
649 *Science Advances*, 5, 1–8, 2019.
- 650 Sun, X.J., and Wang, P.X.: How old is the Asian monsoon system—palaeobotanical records from China, *Palaeogeogr.*
651 *Palaeoclimatol. Palaeoecol.*, 222, 181–222, 2005.
- 652 Sun, Z., Yang, Z.Y., Pei, X.H., Wang, X.S., Yang, T.S., Li, W.M., and Yuan, S.H.: Magnetostratigraphy of Paleogene
653 sediments from northern Qaidam Basin, China: implications for tectonic uplift and block rotation in northern Tibetan
654 plateau, *Earth Planet. Sci. Lett.*, 237, 635–646, 2005.
- 655 Sun, Z.C., Feng, X.J., Li, D.M., Yang, F., Qu, Y.H., and Wang, H.J.: Cenozoic Ostracoda and palaeoenvironments of the
656 northeastern Tarim Basin western China, *Palaeogeogr. Palaeoclimatol. Palaeoecol.* 148, 37–50, 1999.
- 657 Tarasov, P.E., Cheddadi, R., Guiot, J., Bottema, S., Peyron, O., Belmonte, J., Ruiz-sanchez, V., Saadi, F., and Brewer, S.: A
658 method to determine warm and cool steppe biomes from pollen data; application to the Mediterranean and Kazakhstan



- 659 regions, *J. Quat. Sci.*, 13, 335–344, 1998.
- 660 Valdes, P.J., Lin, D., Farnsworth, A., Spicer, R.A., Li, S.H. and Tao, S.: Comment on “Revised paleoaltimetry data show low
661 Tibetan Plateau elevation during the Eocene”, *Science*, 365(6459), eaax8474, 2019.
- 662 Wang, C.S., Zhao, X.X., Liu, Z.Z., Peter, C., Stephan, A.G., Robert, S.C., Zhu, L.D., Liu, S., and Li, Y.L.: Constraints on the
663 early uplift history of the Tibetan Plateau, *P. Natl. Acad. Sci. USA.*, 105, 4987–4992, 2008.
- 664 Wang C.S., Dai, J.G., Zhao, X.X., Li, Y.L., Graham, S.A., He, D.F., Ran, B., and Meng, J.: Outward-growth of the Tibetan
665 Plateau during the Cenozoic: A review, *Tectonophysics*, 621, 1–43, 2014.
- 666 Wang, C.W., Hong, H.L., Li, Z.H., Yin, K., Xie, J., Liang, G.J., Song, B., Song, E., Zhang, K.X.: The Eocene–Oligocene
667 climate transition in the Tarim Basin, Northwest China: evidence from clay mineralogy, *Appl. Clay. Sci.*, 74, 10–19,
668 2013.
- 669 Wang, D., Sun, X.Y., and Zhao, Y.: Late Cretaceous to Tertiary palynofloras in Xingjiang and Qinghai China, *Rev.*
670 *Palaeobot. Palynol.*, 65, 95–104, 1990a.
- 671 Wang, D., Sun, X.Y., Zhao, Y., He, Z.: Palynoflora from Late Cretaceous to Tertiary in Some Regions of Qinghai and
672 Xinjiang, China Environmental Science Press, Beijing, pp. 1–179, 1990b. (in Chinese with English abstract).
- 673 Wang, J., Wang, Y.J., Liu, Z.C., Li, J.Q., and Xi, P.: Cenozoic environmental evolution of the Qaidam Basin and its
674 implications for the uplift of the Tibetan Plateau and the drying of central Asia, *Palaeogeogr. Palaeoclimatol.*
675 *Palaeoecol.*, 152, 37–47, 1999.
- 676 Wang, S.F., Yi, H.S., and Wang, C.S.: Sedimentary facies and palaeogeography features of Nangqian Tertiary basin in Yushu
677 district, Qinghai, *Northwestern Geol.*, 34, 64–67, 2001. (in Chinese, with English abstract).
- 678 Wang, S.F., Yi, H.S., and Wang, C.S.: Sediments and structural features of Nangqian Tertiary Basin in eastern of Tibet-
679 Qingzang Plateau, *Acta Sci. Nat. Univ. Pekin.*, 38, 109–114, 2002. (in Chinese, with English abstract).
- 680 Wang Z.: A new Permian gnetalean cone as fossil evidence for supporting current molecular phylogeny, *Ann. Bot.*, 94, 281–
681 288, 2004.



- 682 Wang, Z.X., Shen, Y.J., and Pang, Z.B.: Three main stages in the uplift of the Tibetan Plateau during the
683 Cenozoic period and its possible effects on Asian aridification: A review, *Clim. Past Discuss.*,
684 <https://doi.org/10.5194/cp-2018-64>, 2018.
- 685 Wei, H.C., Fan, Q.S., Zhao, Y., Ma, H.Z., Shan, F.S., An, F.Y., and Yuan, Q.: A 94-10 Ka pollen record of vegetation change
686 in Qaidam Basin, northeastern Tibetan Plateau, *Palaeogeogr. Palaeoclimatol. Palaeoecol.*, 431, 43–52, 2015.
- 687 Wei, M.: Eocene ostracods from Nangqen in Qinghai. Contribution to the Geology of the Qinghai-Xizang (Tibet) Plateau,
688 17, 313–324, 1985. (in Chinese with English abstract). Geological Publishing House, Beijing
- 689 Wei, Y., Zhang, K., Garzzone, C.N., Xu, Y.D., Song, B., Ji, J.L.: Low palaeoelevation of the northern Lhasa terrane during
690 late Eocene: Fossil foraminifera and stable isotope evidence from the Gerze Basin, *Sci. Rep.*, 6, 27508, 2016.
- 691 Xia, L.Q., Li, X.G., Ma, Z.P., Xu, X.Y., and Xia, Z.C.: Cenozoic volcanism and tectonic evolution of the Tibetan plateau,
692 *Gondwana. Res.*, 19, 850–866, 2011.
- 693 Xiao, G.Q., Abels, H.A., Yao, Z.Q., Dupont-Nivet, G., and Hilgen, F.J.: Asian aridification linked to the first
694 step of the Eocene-Oligocene climate Transition (EOT) in obliquity-dominated terrestrial records (Xining
695 Basin, China), *Clim. Past*, 6, 501–513, 2010.
- 696 Xu, Q., Ding, L., Zhang, L.Y., Cai, F.L., Lai, Q.Z., Yang, D., and Zeng, J.L.: Paleogene high elevations in the Qiangtang
697 Terrane, central Tibetan Plateau, *Earth Planet. Sci. Lett.*, 362, 31–42, 2013.
- 698 Xu, R., Song, Z.C., and Zhou, H.Y., The palynological assemblages in Tertiary sediments of Qaidam Basin and its
699 significance in geology, *Acta. Palaeontol. Sin.*, 6, 429–440, 1958 (in Chinese).
- 700 Xu, Y., Bi, X.W., Hu, R.Z., Chen, Y.W., Liu, H.Q., and Xu, L.L.: Geochronology and geochemistry of Eocene potassic felsic
701 intrusions in the Nangqian basin, eastern Tibet: Tectonic and metallogenic implications, *Lithos.*, 246–247, 212–227,
702 2016.
- 703 Yang, Y.: Systematic and Evolution of *Ephedra* L. (Ephedraceae) from China. PhD Thesis. Institute of Botany Chinese
704 Academy of Sciences, Beijing, 231 pp. 2002. (in Chinese with English summary).



- 705 Yin, A., and Harrison, T.M.: Geologic evolution of the Himalayan–Tibetan orogeny, *Annu. Rev. Earth. Pl. Sc.*, 28, 211–280,
706 2000.
- 707 Yuan, Q., Vajda, V., Li., Q.K., and Shan, F.S.: A late Eocene palynological record from the Nangqian Basin, Tibetan Plateau:
708 Implications for stratigraphy and paleoclimate, *Palaeoworld*, 26: 369–379, 2017.
- 709 Yuan, Q., Barbolini, N.: “Supplementary dataset: Aridification signatures from middle–late Eocene pollen indicate
710 widespread drying across the Tibetan Plateau after 40 Ma”, *Mendeley Data*, V3, doi: 10.17632/xvp68wsd2p.3, 2020.
- 711 Yuan, Q., Barbolini, N., Ashworth, L., Rydin, C., Gao, D.L., Wei, H.C., Fan, Q.S., Qin, Z.J., Du, Y.S., Shan, J.J., Shan, F.S.,
712 and Vajda, V.: Palaeoenvironmental changes in Eocene Tibetan lake systems traced by geochemistry and sedimentology,
713 *Terra Nova*, in prep.
- 714 Zachos, J., Pagani, M., Sloan, L., Thomas, E., and Billups, K.: Trends, rhythms, and aberrations in global climate 65 Ma to
715 present, *Science*, 292, 686–693, 2001.
- 716 Zhang, J., Santosh, M., Wang, X., Guo, L., Yang, X., and Zhang, B.: Tectonics of the northern Himalaya since the India–Asia
717 collision, *Gondwana. Res.*, 21, 939–960, 2012.
- 718 Zhang, W.L.: The high precise Cenozoic magnetostratigraphy of the Qaidam Basin and uplift of the Northern Tibetan
719 plateau, (PhD Thesis). Lanzhou University, Lanzhou, 109 pp, 2006.
- 720 Zhao, Y., Herzschuh, U.: Modern pollen representation of source vegetation in the Qaidam Basin and surrounding
721 mountains, north-eastern Tibetan Plateau, *Veg. Hist. Archaeobot.*, 18, 245–260, 2009.
- 722 Zhou, X.Y., and Li, X.Q.: Variations in spruce (*Picea* sp.) distribution in the Chinese Loess Plateau and surrounding areas
723 during the Holocene, *Holocene*, 22, 687–696, 2011.
- 724 Zhu, H.C., Ouyang, S., Zhan, J.Z., and Wang, Z.: Comparison of Permian palynological assemblages from the Junggar and
725 Tarim Basins and their phytoprovincial significance, *Rev. Palaeobot. Palynol.*, 136, 181–207, 2005.
- 726 Zhu, L., Zhang, H.H., Wang, J.H., Zhou, J.Y., and Xie, G.H.: $^{40}\text{Ar}/^{39}\text{Ar}$ chronology of high-K magmatic rocks in Nangqian
727 Basin at the northern segment of the Jinsha-Red River Shear Zone (JRRSZ), *Geotecton. et Metallog.*, 30, 241–247,



- 728 2006. (in Chinese, with English abstract).
- 729 Zhu, Z.H., Wu, L., Xi, P., Song, Z.C., and Zhang, Y.Y.: A Research on Tertiary Palynology from the Qaidam Basin, Qinghai
- 730 Province, Petroleum Industry Press, Beijing, 1–297, 1985. (in Chinese with English abstract).
- 731